Article

Bioinformatics Analysis Confirms the Target Protein Underlying Mitotic Catastrophe of 4T1 Cells under Combinatorial Treatment of PGV-1 and Galangin

Nurul Awali Fauziyah Hasbiyani [1,2], Febri Wulandari [2], Eri Prasetyo Nugroho [2], Adam Hermawan [2,3] and Edy Meiyanto [2,3,*]

[1] Department of Biotechnology, Graduate School, Universitas Gadjah Mada, Yogyakarta 55281, Indonesia; nurul.awali@ugm.mail.ac.id
[2] Cancer Chemoprevention Research Center, Faculty of Pharmacy, Universitas Gadjah Mada, Yogyakarta 55281, Indonesia; febri.wulandari@mail.ugm.ac.id (F.W.); eri.prasetyo.nugroho@mail.ugm.ac.id (E.P.N.); adam_apt@ugm.ac.id (A.H.)
[3] Macromolecular Engineering Laboratory, Department of Pharmaceutical Chemistry, Faculty of Pharmacy, Universitas Gadjah Mada, Yogyakarta 55281, Indonesia
*   Correspondence: edy_meiyanto@ugm.ac.id; Tel.: +62-274-543120

Abstract: Pentagamavunon-1 (PGV-1), a potential chemopreventive agent with a strong cytotoxic effect, modulates prometaphase arrest. Improvement to get higher effectiveness of PGV-1 is a new challenge. A previous study reported that the natural compound, galangin, has antiproliferative activity against cancer cells with a lower cytotoxicity effect. This study aims to develop a combinatorial treatment of PGV-1 and galangin as an anticancer agent with higher effectiveness than a single agent. In this study, 4T1, a TNBC model cell, was treated with a combination of PGV-1 and galangin. As a result, PGV-1 and galangin showed a cytotoxic effect with IC50 values of 8 and 120 μM, respectively. Combining those chemicals has a synergistic impact, as shown by the combination index (CI) value of 1. Staining with the May Grunwald-Giemsa reagent indicated mitotic catastrophe evidence, characterized by micronuclear and multinucleated morphology. Moreover, the senescence percentage was higher than the single treatment. Furthermore, bioinformatics investigations showed that PGV-1 and galangin target CDK1, PLK1, and AURKB, overexpression proteins in TNBC that are essential in regulating cell cycle arrest. In conclusion, the combination of PGV-1 and galangin exhibit a synergistic effect and potential to be a chemotherapeutic drug by the mechanism of mitotic catastrophe and senescence induction.

Keywords: galangin; PGV-1; TNBC; mitotic catastrophe; senescence

1. Introduction

The National Cancer Institute has tested about 3000 plant species for anticancer therapeutic potential [1]. Galangal (*Alpinia galanga* L.) is one of them, and its bioactive chemical, galangin, could prevent cancer development [2]. Galangin restrains the proliferation of various types of cancer cells through a variety of pathways. Galangin elicits cell death in the ovarian cancer cells models, namely A2780/CP70 and OVCAR-3 [3]. Galangin-induced apoptosis could be initiated by increasing ROS generation. Galangin also inhibits cancer cell cycle progression by downregulating cell cycle proteins machinery [4]. In addition, galangin treatment on LuminalA breast cancer cell MCF-7 and T47D resulting in lowering cell population. Apoptosis on those cells was characterized by the increasing CL-caspase 3, CL-caspase 9, and Bax protein. In another study, galangin regulated cell-cycle-associated proteins, causing cell cycle arrest in MCF-7 cells. Galangin also performs the advantage of being selective for normal cells [5].

Galangin seems to have the ability to stop the proliferation of another type of breast cancer, especially for TNBC subtypes. Despite all that evidence, galangin exhibits relatively

low cytotoxic activity that is not preferable to be considered as a chemotherapeutic agent. Since it is safer for normal cells, galangin may be used in combinatorial therapy with standard cancer chemotherapy. For further application, galangin needs to be combined with another anticancer agent to support its efficacy against cancer cells. Galangin increases the cytotoxic activities of imatinib mesylate against K562 leukemia cells [6]. Galangin also decreased the cardiotoxicity of doxorubicin, a chemotherapeutic drug commonly used in TNBC subtypes [7]. In addition, galangal (Kaempferia galanga) ethanolic extract performs synergistically with doxorubicin against 4T1 cells and reduces oxidative stress in normal cells [8].

We have developed a new anticancer candidate, namely pentagamavunon-1 (PGV-1), a monocarbonyl curcumin analog with strong cytotoxic activities against several cancer cell lines, including 4T1 cells, a mouse TNBC cell line, and an in vivo model [9,10]. PGV-1 showed an excellent cytotoxic effect via apoptosis, induction of senescence, ROS generation, and cell cycle arrest [9,11]. PGV-1 also performed high cytotoxic selectivity on several cancer cells rather than normal cells and did not show toxic evidence in animal models [11]. However, the cytotoxic activity of PGV-1 still needs to be improved. Considering the potency of PGV-1, the targeted molecule in 4T1 cells needs to be explored in more detail. Galangin is proposed to be the candidate of PGV-1 combinatorial treatment in TNBC to improve PGV-1 effectiveness.

Triple-negative breast cancer (TNBC) differed to other breast cancer subtypes in its lacking expression of estrogen receptors (ER), progesterone receptors (PR), and human epidermal growth factor (HER-2) receptors [12]. As a result of the lack of expression of a specific receptor, chemotherapy with nonspecific targets is the first-line treatment for TNBC [13]. Furthermore, combining PGV-1 with other anticancer drugs such as 5-FU and doxorubicin improves its cytotoxic activities [14,15]. Combining two (or more) anticancer drugs is a frequent way to improve the effectiveness of cancer treatment. Because lower chemotherapy doses can be used in combination treatment, systemic toxicity from chemotherapy may be reduced. This has led us to explore the cytotoxic effects of galangin in combination with PGV-1 to enhance the efficacy of PGV-1's anticancer properties. In this work, we evaluated the cytotoxic effects of galangin and its combination with PGV-1 and induction of mitotic catastrophe. The protein targets of galangin and PGV-1 in TNBC, its expression, and the patient's survival rate were also explored through bioinformatics analysis. In addition, molecular docking was employed to identify the inhibitory effect of galangin and PGV-1 in the TNBC protein targets. Hopefully, all the data reveal the molecular basis of the synergistic effect of PGV-1 and galangin on TNBC cells.

2. Materials and Methods

2.1. Cells Culture

The 4T1 was obtained from Professor Masashi Kawaichi, Nara Institute of Science and Technology, Japan. The cells were maintained in Dulbecco's modified Eagle medium (DMEM) high glucose (Gibco, Carlsbad, CA, USA) supplemented with 10% *v/v* fetal bovine serum (FBS) (Sigma, St. Louis, MO, USA). 150 IU/mL penicillin, and 150 μg/mL streptomycin (Gibco, Grand Island, NY, USA).

2.2. PGV-1 and Galangin

Cancer Chemoprevention Research Center (CCRC), Faculty of Pharmacy, Universitas Gadjah Mada, provided the PGV-1 with 95% purity. Galangin was obtained from Sigma Chemical Co. (St. Louis, MO, USA).

2.3. Sample Preparation

Each PGV-1 and galangin solution was dissolved in dimethylsulfoxide (DMSO) in a stock solution at a concentration of 0.1 μM. Each solution is then diluted by DMEM in a series of concentrations.

2.4. Cytotoxicity Assay

Cells were grown into each well of a 96-well plate at a concentration of 8×10^3 cells/mL. Then, cells were treated with various concentrations of galangin, PGV-1, or its combination for 24 h. After incubation, cells were washed in phosphate buffer saline (PBS) (Sigma). Each well got an additional 100 mL of MTT reagent (Sigma) diluted in DMEM (1:9) for 4 h. The 10% sodium dodecyl sulfate (SDS) was added to stop the reaction and incubated overnight, followed by the absorbance measurement at 595 nm under a microplate reader.

2.5. MayGrünwald-Giemsa Staining

8×10^4 4T1 cells/well cells were seeded on 6-well plates and treated with various concentrations of galangin, PGV-1, and its combination for 24 h. Then, cells were washed with 1 mL of PBS $1\times$ (pH 7) and received 200 μL of May-Grünwald Stain solution. After that, each well was added by 1 mL of phosphate buffer saline $1\times$ in 5 min. Following that, each well was given a diluted Giemsa solution (1:20 v/v) with 200 μL. Next, the cells were washed with 200 μL deionized water and dried in the open air. Observation of cells was carried out by inverted microscopy and documented with a camera.

2.6. Senescence-Associated β-Galactosidase Assay

In total, 8×10^4 4T1 cells/well cells were distributed on 6-well plates, incubated with several concentrations of galangin, PGV-1, and its combination for 24 h. After PBS washing, the cells were fixed with 2% formaldehyde -0.2% glutaraldehyde for 10 min and then washed again using PBS $1\times$. Cells staining was performed by using X-gal solution, 40 mM PBS $2\times$ (pH 6.0), 5 mM $K_4Fe(CN)_6$, 5 mM $K_3Fe(CN)_6$, and 2 mM $MgCl_2$. Following the incubation, for 3 days, the stained cells were observed under an inverted microscope ($100\times$ magnification). The β-D-galactosidase positive cells were characterized by green color and then quantified using ImageJ software.

2.7. Statistical Analysis

All data are represented as means, standard deviations, or standard errors. The one-way ANOVA analysis of variance was used to analyze the experimental data, followed by Tukey post hoc analysis in SPSS (SPSS Inc., Chicago, IL, USA, version 21). Significant p values were less than 0.05.

2.8. Target Prediction of Galangin and PGV-1 in TNBC

SwissTargetPrediction [16] provides 376,342 compounds and 3068 macromolecular targets in the database that predicted the most likely protein targets of small molecules [17]. This website was used to predict the protein target of galangin and PGV-1. The protein target was then compared to TNBC overexpressed genes using interactivenn [18].

2.9. UALCAN Analysis

Ualcan [19], an online public database of microarray profiles and next-generation sequencing, was used to examine the KIF11, CDK1, PLK1, and AURKB gene expression across breast cancers and normal tissues as well as in various subgroups such as cancer subtypes. All statistical data were taken directly from the corresponding database.

2.10. Oncolnc Database Analysis

The Oncolnc database [20], an open-access web-based platform, was employed to analyze the lncRNA expression from transcriptome concerning survival rate [21]. A dataset containing 21 cancer studies from more than 8000 patients was mined through this tool's algorithm to investigate the relative overall survival in breast cancer patients' overexpression of CDK1, PLK1, and AURKB. The significant differences of the survival between two different level of expression were determined based on the statistical calculation provided by the platform.

2.11. Molecular Docking

To validate the binding interaction between galangin and PGV-1 toward KIF11, CDK1, PLK1, and AURKB, we conducted a molecular docking analysis using a licensed software MOE 2010.10 for the Faculty of Pharmacy UGM. A computational study was presented to simulate molecular binding, calculate RMSD, and visualize protein–ligand interaction. The PDB ID of KIF11, CDK1, PLK1, and AURKB, were 2YAC, 2VGO, 6GU6, 3ZCW, respectively. The placement setting and scoring method utilized the triangle matcher and London. The docking results from 10 retain settings were refined using the force field method. ChemDraw software (version 2 1. 7.0) was used to draw the chemical structure of galangin and PGV-1 and then minimized the structural energy and generated for conformational structure in MOE. The molecular docking study was managed on the native ligand binding site of each protein. The output of the molecular docking explicated the affinity represented by the docking score and the binding visualization of each compound to the target proteins.

3. Results

3.1. Anti-Proliferative Activity of Galangin and PGV-1 in TNBC

Anti-proliferative activity of galangin and PGV-1 was tested by MTT assay. Cells were incubated in the absence and presence of PGV-1 (0.5–16 μM concentration) and galangin (10–1000 μM concentration), resulting in suppression of viable cells depending on the solution concentration (Figure 1a,b). The antiproliferative activity was expressed in IC50 (a dose capable of inhibiting 50% of cell growth), respectively, as the IC50 value of galangin and PGV-1 on 4T1 cells was 120 and 8 μM (Table 1). Interestingly, combination treatment of both compounds reduced 4T1 cell viability better than single therapy (Figure 1c). These CI values scored less than 1 indicate that the cotreatments have synergistic properties (Table 2). These synergistic effects might be affected by different molecular events of each component that lead to physiological phenomena.
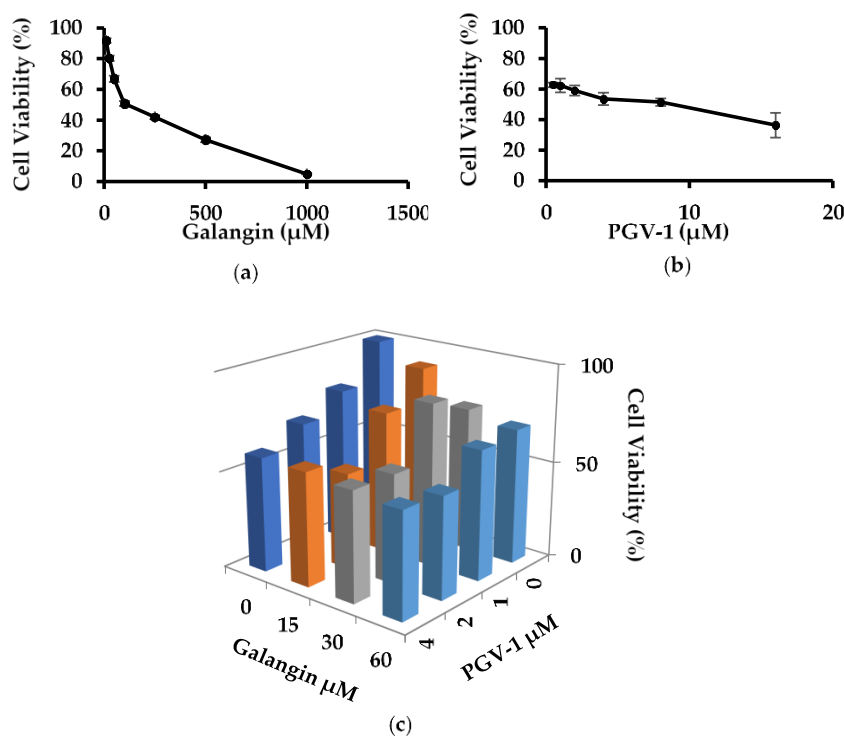

Figure 1. Cytotoxic effects of (**a**) galangin, (**b**) PGV-1, and (**c**) combination of galangin and PGV-1 in 4T1 cells (Dark blue: PGV-1 only; Orange: Galangin 15 μM + serial concentration of PGV-1; Grey: Galangin 30 μM + serial concentration of PGV-1; Light Blue: Galangin 60 μM + serial concentration of PGV-1. Cell viability was determined by using an MTT assay.

Table 1. IC$_{50}$ of galangin and PGV-1 on 4T1 cells.

Compound	IC$_{50}$ (µM)
Galangin	120
PGV-1	8

Table 2. CI of galangin and PGV-1 combination on 4T1 cells.

Galangin (µM)	PGV-1 (µM)		
	1	2	4
15	−0.13	0.03	−0.24
30	0.12	0.10	0.04
60	0.56	0.20	0.06

3.2. Effect of Galangin and PGV-1 on Cell Cycle

PGV-1 was able to induce cycle arrest of leukemia cell K562 in prometaphase [18]. This study explored galangin and PGV-1 effect in modulation cell cycle arrest in TNBC 4T1 cells carried out by morphological observation. The 4T1 cells were stained by the May Grünwald-Giemsa reagent to observe nuclear changes. Treatment of 4T1 breast cancer cells with single PGV-1 or its co-treatment with galangin resulted in mitotic catastrophe phenomena characterized by enlargement cell size (compared to the control cell), small and numerous cell nuclei (micronuclear and polynuclear), shown by yellow arrows (Figure 2a). By contrast, galangin treatment showed different results. In addition, 4T1 cells treated with PGV-1 4 µM and galangin 60 µM increased the population of mitotic catastrophe (17%) compared to PGV-1 4 µM alone (11%) (Figure 2b). As a result, galangin and PGV-1 work synergistically to increase the occurrence of mitotic catastrophe in 4T1 breast cancer cells.
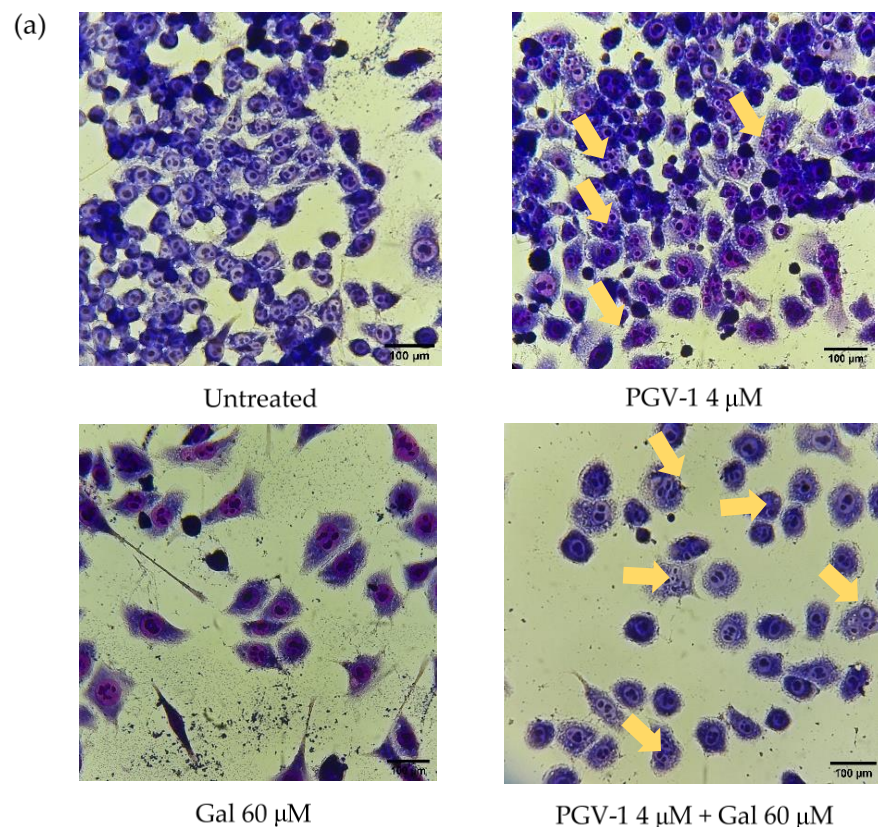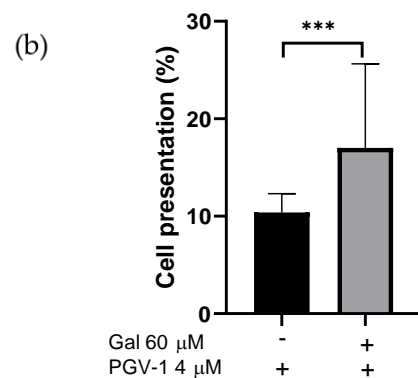
(a)

Untreated

PGV-1 4 µM

Gal 60 µM

PGV-1 4 µM + Gal 60 µM

Figure 2. *Cont.*

(b)

Figure 2. May-Grunwald Giemsa staining on 4T1 cells. (**a**) The morphology of cells was observed under an inverted microscope. (**b**) The percentage of Mitotic catastrophe was determined after treatment. Data are expressed as mean ± SD of three independent experiments. *** $p < 0.01$.

3.3. Galangin and Its Combination with PGV-1 Induces Cell Senescence

Furthermore, the potential of the PGV-1, galangin, and their combination in inducing senescence in PGV-1 breast cancer cells was investigated using the senescence-associated β-galactosidase (SA-β-Gal) assay method. Senescence cells are marked with a green color, pointed by the red arrow (Figure 3a). Treatment with PGV-1 at 4 μM concentration induced higher senescence than control cells. The senescence of 4T1 cells in the 4 μM concentration of PGV-1 compound treatment increased by 2% compared to control cells. In this experiment, doxo was used as a positive control as well as a known senescence-inducing agent. Doxorubicin treatment with a concentration of 100 nM was able to induce senescence 10% higher than cell control.
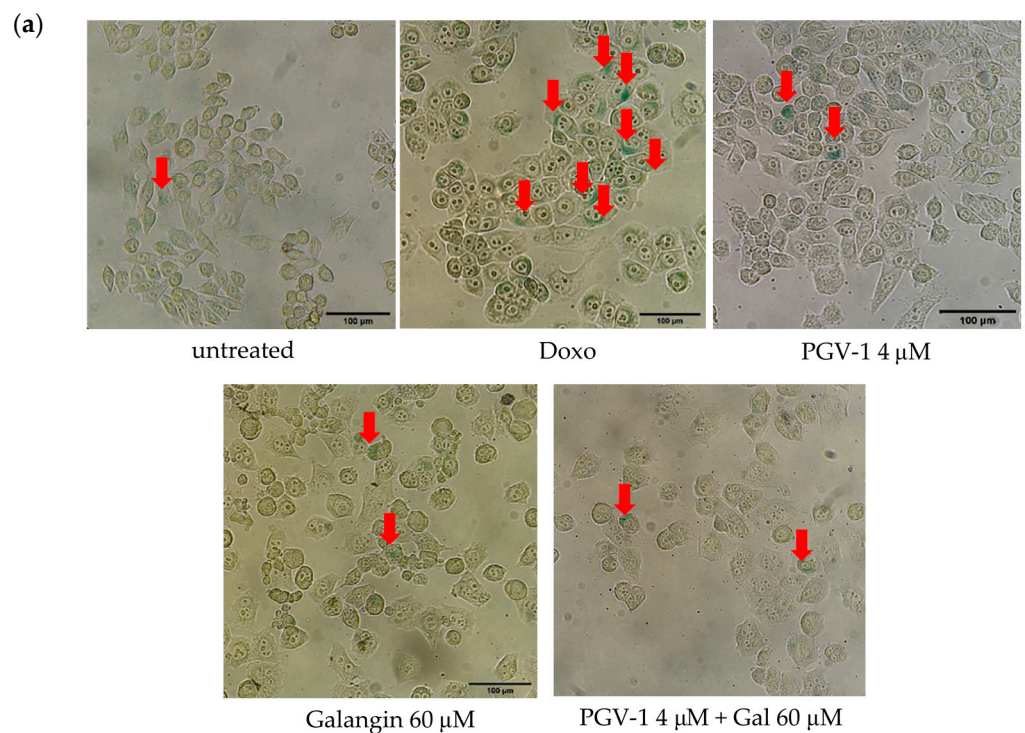
(**a**)

untreated   Doxo   PGV-1 4 μM

Galangin 60 μM   PGV-1 4 μM + Gal 60 μM
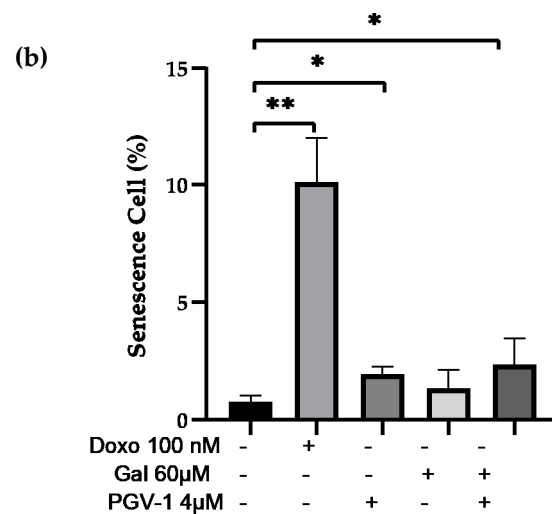
Figure 3. *Cont.*

Figure 3. Induction of senescence in 4T1 cells following galangin and PGV-1 treatment. Senescence cells were analyzed using the SA-β-galactosidase staining assay. (**a**) The morphology of cells was observed after 72 h staining under an inverted microscope. (**b**) The percentage of senescent cells was determined after treatment. Data are expressed as mean ± SD of three independent experiments. * $p < 0.05$, ** $p < 0.01$.

3.4. Galangin and PGV-1 Target Proteins Prediction on TNBC

To find out the TNBC target protein of PGV-1 and galangin, an exploration was carried out through the website SwissTargetPrediction [16]. Moreover, a comprehensive search via UALCAN website resulted in 243 proteins are upregulated in TNBC. We generated a Venn diagram between those three data and resulted in seven proteins are galangin molecular targets in TNBC: PLK-1, AURKB, CDK1, CCNB1, CCNB2, TOP2A, and NEK2 (Table 3). While six proteins are targeted by PGV-1 in TNBC: KIF11, CHEK1, CCNE1, QPCT, CDK1, and TOP2A (Table 4) (Figure 4).

Table 3. Role and function of galangin target proteins.

Protein	Role	Function	Reference
PLK-1	Protein Kinase	chromosome segregation, spindle assembly and cytokinesis	[22]
AURKB	Protein Kinase	chromosome-microtubule attachment	[23]
CDK1	Protein Kinase	G2/M regulator	[24]
CCNB1	Subunit regulator CDK1	G2/M regulator	[25]
CCNB2	Subunit regulator CDK1	G2/M regulator	[25]
TOP2A	Enzim Katalis	Chromosome separation and DNA replication	[26]
NEK2	Protein Kinase	Chromosome duplication and separation	[27]

Table 4. Role and function of PGV-1 target proteins.

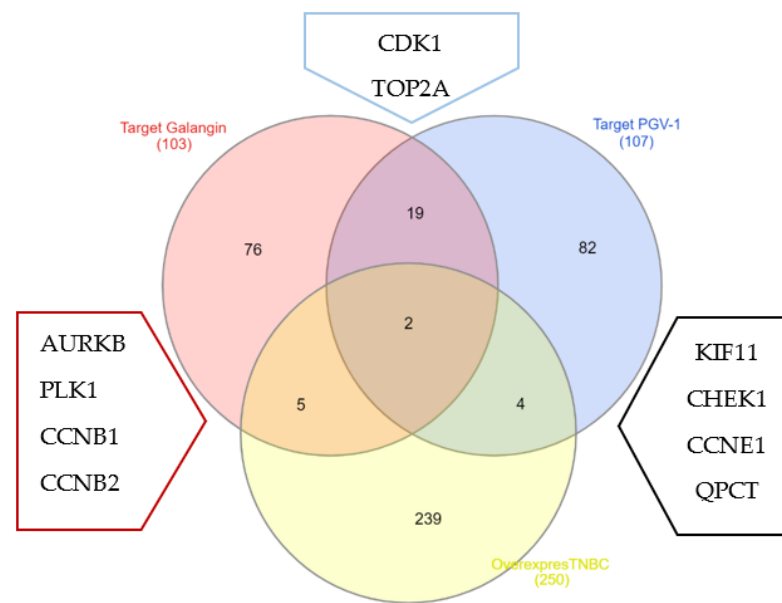| Protein	Role	Function	Reference
CDK1	Protein Kinase	G2/M regulation	[24]
TOP2A	Enzim Katalis	Chromosome separation and DNA replication	[26]
KIF11	Enzim Katalis	Forms bioplar mitotic spindles	[28]
CHK1	Protein Kinase	DDR mediator	[29]
CCNE1	Protein Kinase	G1/S regulator	[30]
QPCT	Enzim	Biosynthesis of piroglutamil peptida	[27]

Figure 4. Venn diagram of predictive target protein for PGV-1 and galangin compounds with protein overexpression in TNBC breast cancer. Prediction of target protein compounds PGV-1 and galangin obtained from the website of the Swiss target prediction protein. TNBC breast cancer overexpression proteins were obtained from the TCGA database from the UALCAN website.

Protein's target of galangin and PGV-1 mostly play an important role, either interphase or mitotic phase in cell cycle progression. In interphase, TOP2A regulates DNA double-helix separation in S phase [26], while CCNE1 controls the shifting from G1 to S phase [30]. Moreover, mitotic entrance and progression were regulated by PLK-1 [22], CDK1 [24], CCNB1 [25], AURKB [23], KIF 11 [28], TOP2A [26], and NEK2 [27] proteins. Moreover, activation of CHK1 responds in a mitotic perturbation or usually called mitotic checkpoint [29].

3.5. Expression of CDK1, PLK-1, and AURKB in Breast Cancer

We initially evaluated three essential mitotic regulator proteins: CDK1, PLK-1, and AURKB transcription levels in multiple cancers from TCGA. Figure 5 shows that the expression of those proteins was significantly higher in breast cancer cells. Furthermore, the expressions of CDK1, PLK-1, and AURKB among various breast cancers show higher expression in breast cancers with the TNBC subtype.

3.6. Kaplan–Meier Survival Analysis

The higher expression of these three proteins exhibited an impact on patient survival. The Kaplan–Meier plot displayed the survival of the samples with high CDK1, PLK-1, and AURKB expression (red line) versus survival times. The result indicates that patients with low protein expression levels had significantly better overall survival rates than the opposite group (Figure 6).
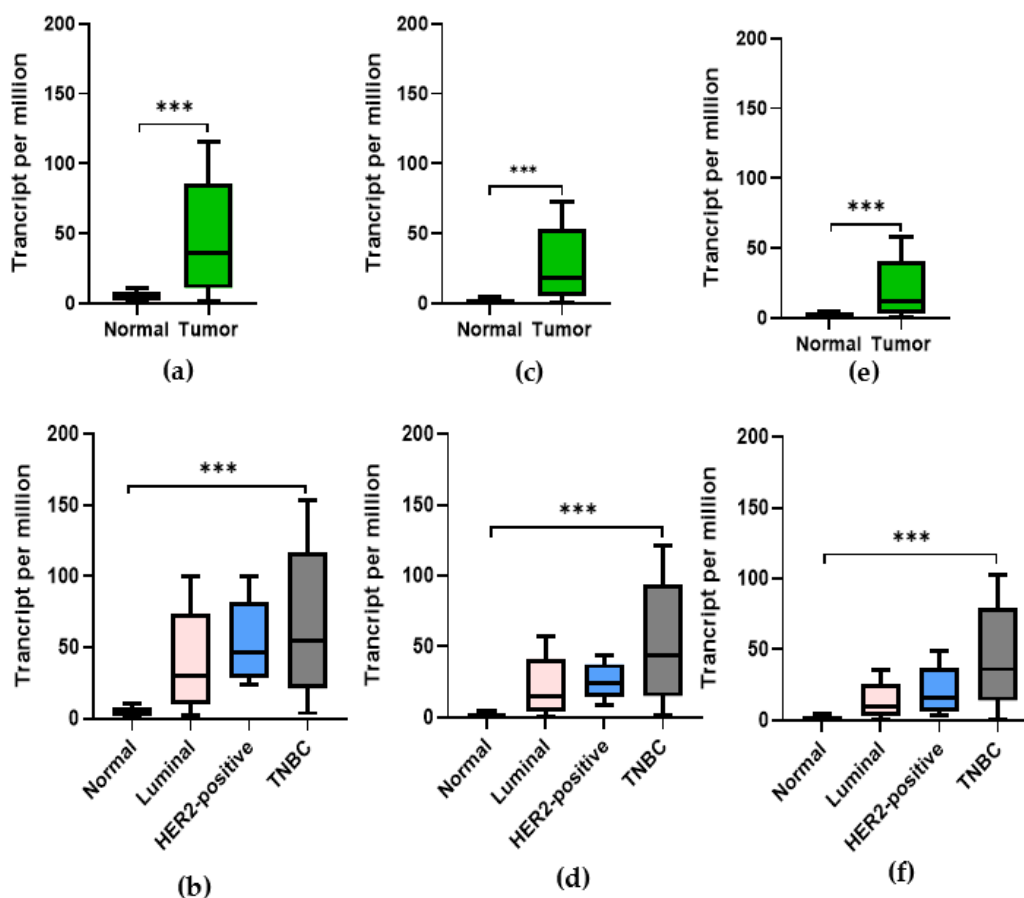
Figure 5. Expression of TNBC protein marker in normal cell, tumor cell, and various types of breast cancer cells, (**a,b**) CDK1 (*p* value 1×10^{-12}), (**c,d**) PLK1 (*p* value 1.62×10^{-12}), (**e,f**) AURKB (*p*-value 1.62×10^{-12}). TCGA database is obtained through the UALCAN website. *** $p < 0.01$.
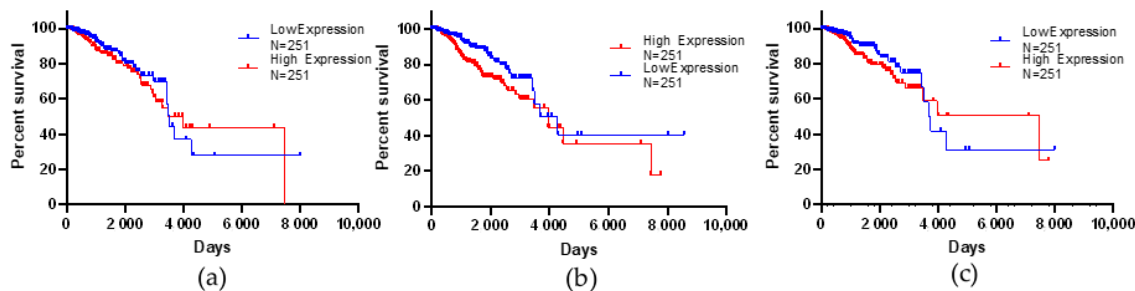

Figure 6. Percent survival of breast cancer patients with over- and under-expression of target proteins. (**a**) Percent survival of patients with high and low CDK1 expression. *p*-value 0.048. (**b**) Percent survival of patients with high and low PLK1 expression. *p*-value = 0.0252, and (**c**) percentage of survival of patients with high and low AURKB expression. *p*-value 0.214. The TCGA dataset can be accessed via the Oncoln website.

3.7. Molecular Docking

Inhibition of cell cycle process targeting on its molecular mechanism is essential to combat breast cancer proliferation. Following some markers protein involved in cell cycle progression, we then investigate the possible inhibitory activity of galangin and PGV-1 targeting KIF11, CDK1, PLK-1, and AURKB protein through a molecular docking simulation. Native ligands were embedded into Dinaciclib for CDK1, NMS-P937 for PLK-1, Reversine for AURKB, and 4A2 for KIF11, respectively (Figure 7).
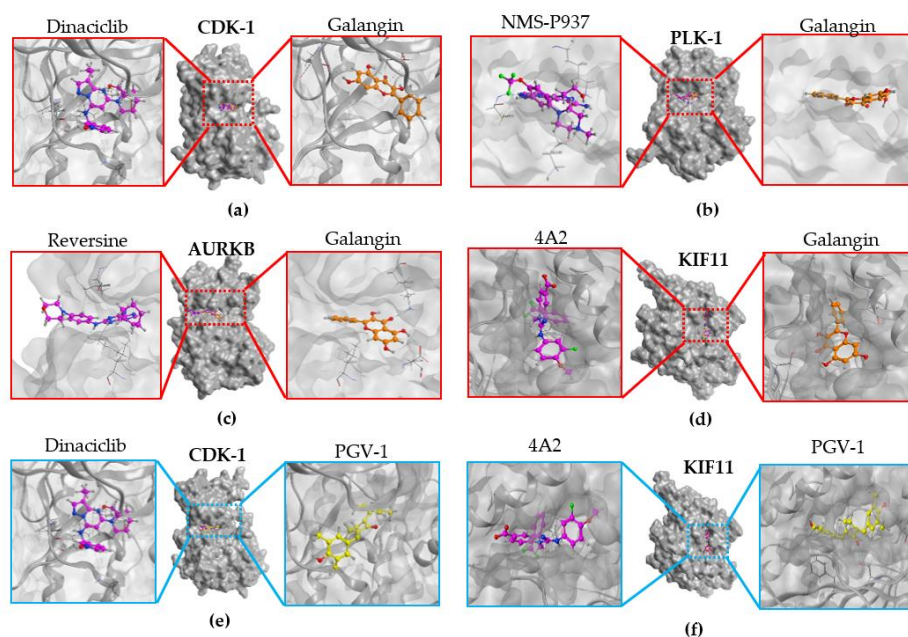
Figure 7. Binding interaction model, (**a**) CDK-1 to its native ligand and galangin, (**b**) of PLK-1 to its native ligand and galangin, (**c**) AURKB to its native ligand and galangin, (**d**) KIF11 to its native ligand and galangin, (**e**) CDK-1 to its native ligand and PGV-1, (**f**) KIF11 to its native ligand and PGV-1.

On CDK1, galangin and PGV-1 showed a slightly lower docking score than Dinaclib, suggesting that CDK1 binds and reacts preferentially with galangin and PGV-1 (Table 5). The higher docking score of galangin, also found on AURKB, suggested a lower binding affinity than that of native ligands Reversine (Table 6). This contrasted with PLK-1 and KIF11, whose galangin docking score was a little higher than its native ligand. Overall, galangin performed a promising inhibitory activity on CDK1 and AURKB, while PGV-1 could target CDK1 protein (Table 6).

Table 5. Docking score of ligands toward PDK-1, CDK-1, AURKB, and KIF11 on galangin.

No.	Protein	PDB ID	Native Ligand		Galangin	
			RMSD (Å)	Docking Score (kcal/mol)	RMSD (Å)	Docking Score (kcal/mol)
1	PLK-1	2YAC	0.8535	−13.9847	0.7247	−13.5717
2	AURKB	2VGO	1.3148	−7.8545	1.7724	−9.0003
3	CDK-1	6GU6	1.2543	−10.8300	1.6107	−12.2080
4	KIF11	3ZCW	0.8005	−13.6193	1.1531	−13.4846

Table 6. Docking score of ligands toward CDK-1 and KIF2A on PGV-1.

No.	Protein	PDB ID	Native Ligand		PGV-1	
			RMSD (Å)	Docking Score (kcal/mol)	RMSD (Å)	Docking Score (kcal/mol)
1	CDK-1	6GU6	1.2543	−10.8300	1.2612	−14.0391
2	KIF11	3ZCW	0.8005	−13.6193	0.8661	−13.3464

4. Discussion

Although a previous study has revealed galangin potency in eliminating the growth of breast cancer cells, no study reported its suppression role in TNBC, a type of breast cancer that has negative expression of ER, PR, and HER-2. We previously found that galangin

induces apoptosis in MCF-7 cells, which belongs to luminal A, a type of breast cancer. This apoptosis process was related to biphasical expression of apoptosis regulator proteins Bcl-2 and Bax. Bcl-2 protein expression was downregulated, while Bax protein expression was increased significantly [4]. Another study published galangin could perform its effects on ROS generation. Exposure galangin to cells increased ROS production associated by apoptosis induction [6]. In this exploration, we characterized galangin, and revealed that galangin could inhibit the proliferation of 4T1, a TNBC cell line. In comparison to ER-breast cancer cell, antiproliferative activity galangin on 4T1 cell (IC50 = 120 μM) was lower than Hs578T cell (IC$_{50}$ = 11 μM) [29]. Interestingly, galangin co-treatment with PGV-1 resulted in a synergistic effect, which could reduce 4T1 viability better than each single compound treatment.

Galangin suppresses cell cycle progression through various phases in the cell cycle: G1, S, or G2/M phase depend on the cancer cell line. Galangin inhibits G0/G1 progression to the S phases. This is supported by the evidence that galangin eliminates cyclin D3 and suppresses the expression of cyclins A and E [29]. Both galangin and PGV-1 are safe for normal cells. Treatment of PGV-1 for 48 h on mouse embryonic fibroblasts (MEFs) cell are counted higher (120%) than leukemic cell K562 (40%) [17]. Moreover, PGV-1 is selective in normal cell HEK293T than breast cancer cell line MCF-7 by selectivity index (SI) scored 5.57 [9]. In addition, galangin also showed its safety in normal cells, human mesangial cells (MC), and mouse renal tubular epithelial (TMCK-1) due to no morphological changes after treatment of 30 μM galangin for 24 h [5]. In addition, PGV-1 provided good stability properties. PGV-1 treatment is stable in leukemic cell K562 after 6 days of removal compound as counted by viability cell less than 5% [17], suggesting that PGV-1 irreversibly prevents the proliferation of the cancer cells. Nevertheless, co-treatment of galangin with PGV-1 on 4T1 and normal cells needs further investigation concerning the time course effectiveness and the safety insurance.

In this experiment, galangin combined with PGV-1 shows a synergistic effect in modulation mitotic arrest in 4T1 cells by the evidence of mitotic catastrophe, which can be observed through May Grünwald-Giemsa staining. Mitotic catastrophe is described as a cell-death-associated process caused by aberrant mitosis characterized with multiple micronuclei [31] and is always followed by mitotic arrest [32]. Micronuclei are caused by fragmented chromosomes that are not distributed among nuclear daughters, where two or more nuclei of heterogeneous size can occur due to equilibration of karyokinesis [33]. Moreover, multinucleated cells are caused by non-condensed clusters of chromosomes undergoing cleavage errors. Another factor that causes multinucleation is multipolar mitosis, which is caused by multicentrosomes, resulting in the withdrawal of chromosomes in four directions [32]. Multinucleation on mitotic catastrophe is caused by inhibition of KIF11 that results in a multipolar spindle, as it targets prediction of PGV-1. Mitotic catastrophe is an important target in cancer cell elimination, especially in breast cancer [34]. Galangin treatment does not allow arrest in the G2/M phase, unlike its combination with or PGV-1 single treatment. This is probably because the galangin target in TNBC was predicted on cyclin B and CDK1, preventing the cell from entering the mitotic phase during the cell cycle. This evidence is supported by a previous study that galangin downregulates cyclin B and CDK1 expression in MCF-7 cells [4].

Galangin primarily targets TNBC cell-cycle-regulating proteins covering PLK-1, AU-RKB, CDK1, CCNB1, CCNB2, TOP2A, and NEK2, while PGV-1 targets KIF11, CHEK1, CCNE1, QPCT, CDK1, and TOP2A (Figure 8). Since those proteins are essential regulators in cell cycle, especially in mitosis machinery, targeting their activity may induce cell cycle arrest in mitosis, leading to mitotic catastrophe [35,36]. This study also realizes that CDK1, PLK-1, and AURKB expression in TNBC is significantly higher than normal cells and elicits a lower survival rate in breast cancer patients. Thus, targeting those proteins is a promising approach in breast cancer medication. In breast cancer (BC) patients, a high expression level of PLK1 was noted as an essential marker for cancer progression and metastasis with a poor prognosis [37,38]. PLK1 involves in G2/M progression. In addition, suppression

of cyclin B1 and cyclin B2 resulted in a mitotic arrest that can be followed by mitotic catastrophe [30]. Mitotic perturbation may also be caused by activation of Chk1, which phosphorylates CDK1 during DNA damage [28]. Hence, this study gives insight into the potential application of co-treatment of galangin and PGV-1 to combat TNBC problems and the expectation to reduce the adverse risk of chemotherapy.
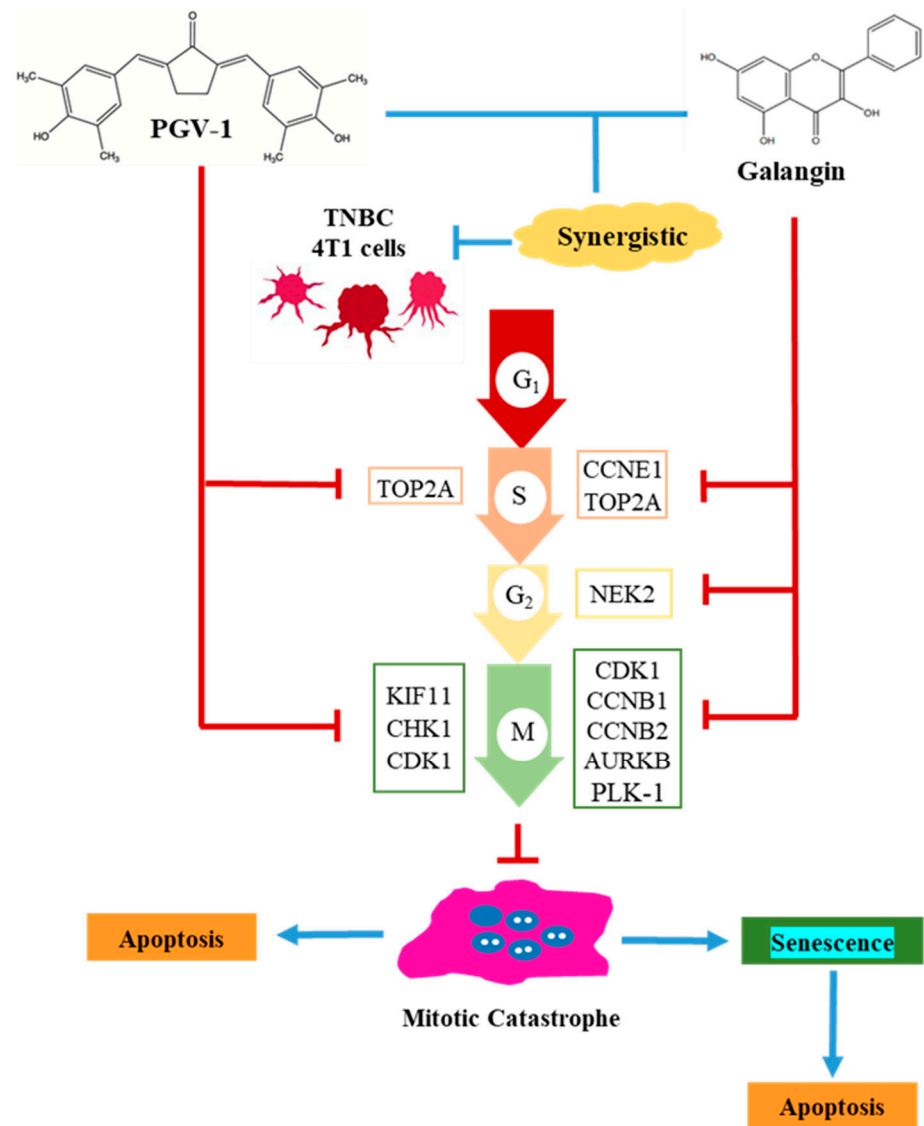

Figure 8. The proposed mechanism of the synergistic effect of PGV-1 and galangin on TNBC 4T1 cells in inducing cells senescence.

5. Conclusions

PGV-1 and galangin combined exhibit a synergistic effect to suppress the cell growth of 4T1 cells through inducing mitotic catastrophe in correlation with increasing cellular senescent. PGV-1 alone induces cellular senescence and mitotic catastrophe TNBC cells suggesting through the interaction of mitotic machinery proteins, namely KIF11, CHEK1, CCNE1, and CDK1. Galangin alone does not induce mitotic catastrophe or cellular senescence, but it enhances the cellular senescence by PGV-1 probably through the interaction with mitotic protein markers, including PLK-1, AURKB, CDK1, CCNB1, and CCNB2. That combination could be promoted as a co-chemotherapeutic treatment against TNBC with furthermore deep exploration.

References

1. Desai, A.; Qazi, G.; Ganju, R.; El-Tamer, M.; Singh, J.; Saxena, A.; Bedi, Y.; Taneja, S.; Bhat, H. Medicinal Plants and Cancer Chemoprevention. *Curr. Drug Metab.* **2008**, *9*, 581–591. [CrossRef]
2. Zou, Y.; Li, R.; Kuang, D.; Zuo, M.; Li, W.; Tong, W.; Jiang, L.; Zhou, M.; Chen, Y.; Gong, W.; et al. Galangin Inhibits Cholangiocarcinoma Cell Growth and Metastasis through Downregulation of MicroRNA-21 Expression. *BioMed Res. Int.* **2020**, *2020*, 5846938. [CrossRef] [PubMed]
3. Ren, K.; Zhang, W.; Wu, G.; Ren, J.; Lu, H.; Li, Z.; Han, X. Synergistic anti-cancer effects of galangin and berberine through apoptosis induction and proliferation inhibition in oesophageal carcinoma cells. *Biomed. Pharmacother.* **2016**, *84*, 1748–1759. [CrossRef]
4. Liu, D.; You, P.; Luo, Y.; Yang, M.; Liu, Y. Galangin Induces Apoptosis in MCF-7 Human Breast Cancer Cells Through Mitochondrial Pathway and Phosphatidylinositol 3-Kinase/Akt Inhibition. *Pharmacology* **2018**, *102*, 58–66. [CrossRef]
5. Song, W.; Yan, C.-Y.; Zhou, Q.-Q.; Zhen, L.-L. Galangin potentiates human breast cancer to apoptosis induced by TRAIL through activating AMPK. *Biomed. Pharmacother.* **2017**, *89*, 845–856. [CrossRef]
6. Tolomeo, M.; Grimaudo, S.; Di Cristina, A.; Pipitone, R.M.; Dusonchet, L.; Meli, M.; Crosta, L.; Gebbia, N.; Invidiata, F.P.; Titone, L.; et al. Galangin increases the cytotoxic activity of imatinib mesylate in imatinib-sensitive and imatinib-resistant Bcr-Abl expressing leukemia cells. *Cancer Lett.* **2008**, *265*, 289–297. [CrossRef]
7. Ravichandra, V.; Hanumantharayappa, B.; Papasani, V. Evaluation of Cardio Protective Activity of Galangin against Doxorubicin Induced Cardiomyopathy. *Int. J. Pharm. Pharm. Sci.* **2014**, *6*, 86–90.
8. Nur, F.N.F.; Nugraheni, N.; Salsabila, I.A.; Haryanti, S.; Da'I, M.; Meiyanto, E.; Ahlina, F.N. Revealing the Reversal Effect of Galangal (*Alpinia galanga* L.) Extract against Oxidative Stress in Metastatic Breast Cancer Cells and Normal Fibroblast Cells Intended as a Co- Chemotherapeutic and Anti-Ageing Agent. *Asian Pac. J. Cancer Prev.* **2020**, *21*, 107–117. [CrossRef]
9. Meiyanto, E.; Putri, H.; Larasati, Y.A.; Utomo, R.Y.; Jenie, R.I.; Ikawati, M.; Lestari, B.; Yoneda-Kato, N.; Nakamae, I.; Kawaichi, M.; et al. Anti-proliferative and Anti-metastatic Potential of Curcumin Analogue, Pentagamavunon-1 (PGV-1), Toward Highly Metastatic Breast Cancer Cells in Correlation with ROS Generation. *Adv. Pharm. Bull.* **2019**, *9*, 445–452. [CrossRef]
10. Meiyanto, E.; Husnaa, U.; Kastian, R.F.; Putri, H.; Larasati, Y.A.; Khumaira, A.; Pamungkas, D.D.P.; Jenie, R.I.; Kawaichi, M.; Lestari, B.; et al. The Target Differences of Anti-Tumorigenesis Potential of Curcumin and its Analogues against HER-2 Positive and Triple-Negative Breast Cancer Cells. *Adv. Pharm. Bull.* **2020**, *11*, 188–196. [CrossRef]
11. Lestari, B.; Nakamae, I.; Yoneda-Kato, N.; Morimoto, T.; Kanaya, S.; Yokoyama, T.; Shionyu, M.; Shirai, T.; Meiyanto, E.; Kato, J.-Y. Pentagamavunon-1 (PGV-1) inhibits ROS metabolic enzymes and suppresses tumor cell growth by inducing M phase (prometaphase) arrest and cell senescence. *Sci. Rep.* **2019**, *9*, 14867. [CrossRef]
12. Fragomeni, S.M.; Sciallis, A.; Jeruss, J.S. Molecular Subtypes and Local-Regional Control of Breast Cancer. *Surg. Oncol. Clin. N. Am.* **2018**, *27*, 95–120. [CrossRef]
13. Chalakur-Ramireddy, N.K.; Pakala, S.B. Combined drug therapeutic strategies for the effective treatment of Triple Negative Breast Cancer. *Biosci. Rep.* **2018**, *38*, BSR20171357. [CrossRef]
14. Hermawan, A.; Fitriasari, A.; Junedi, S.; Ikawati, M. Pgv-0 and Pgv-1 Increased Apoptosis Induction Of Doxorubicin on Mcf-7 Breast Cancer Cells. *Pharmacon* **2011**, *12*, 55–59.
15. Meiyanto, E.; Septisetyani, E.P.; Larasati, Y.A.; Kawaichi, M. Curcumin Analog Pentagamavunon-1 (PGV-1) Sensitizes Widr Cells to 5-Fluorouracil through Inhibition of NF-κB Activation. *Asian Pac. J. Cancer Prev.* **2018**, *19*, 49–56. [CrossRef]
16. SwissTargetPrediction. Available online: http://www.swisstargetprediction.ch/ (accessed on 17 May 2021).
17. Daina, A.; Michielin, O.; Zoete, V. SwissTargetPrediction: Updated data and new features for efficient prediction of protein targets of small molecules. *Nucleic Acids Res.* **2019**, *47*, W357–W364. [CrossRef]
18. Interactivenn. Available online: http://www.interactivenn.net/website (accessed on 21 May 2021).

19. Ualcan. Available online: http://ualcan.path.uab.edu (accessed on 21 May 2021).
20. Oncolnc. Available online: http://www.oncolnc.org/ (accessed on 21 May 2021).
21. Anaya, J. OncoLnc: Linking TCGA survival data to mRNAs, miRNAs, and lncRNAs. *PeerJ Comput. Sci.* **2016**, *2*, e67. [CrossRef]
22. Baran, V.; Brzakova, A.; Rehák, P.; Kovarikova, V.; Solc, P. PLK1 regulates spindle formation kinetics and APC/C activation in mouse zygote. *Zygote* **2015**, *24*, 338–345. [CrossRef]
23. Otto, T.; Sicinski, P. Cell Cycle Proteins as Promising Targets in Cancer Therapy. *Nat. Rev. Cancer* **2017**, *17*, 93–115. [CrossRef]
24. Schatten, H. Mitosis. In *Brenner's Encyclopedia of Genetics*; Academic Press: Waltham, MA, USA, 2013; pp. 448–451. ISBN 978-0-08-096156-9.
25. Gong, D.; Ferrell, J.E. The Roles of Cyclin A2, B1, and B2 in Early and Late Mitotic Events. *Mol. Biol. Cell* **2010**, *21*, 3149–3161. [CrossRef] [PubMed]
26. Wendorff, T.; Schmidt, B.H.; Heslop, P.; Austin, C.A.; Berger, J.M. The Structure of DNA-Bound Human Topoisomerase II Alpha: Conformational Mechanisms for Coordinating Inter-Subunit Interactions with DNA Cleavage. *J. Mol. Biol.* **2012**, *424*, 109–124. [CrossRef]
27. Fang, Y.; Zhang, X. Targeting NEK2 as a promising therapeutic approach for cancer treatment. *Cell Cycle* **2016**, *15*, 895–907. [CrossRef]
28. Swarnkar, S.; Avchalumov, Y.; Raveendra, B.L.; Grinman, E.; Puthanveettil, S.V. Kinesin Family of Proteins Kif11 and Kif21B Act as Inhibitory Constraints of Excitatory Synaptic Transmission Through Distinct Mechanisms. *Sci. Rep.* **2018**, *8*, 17419. [CrossRef]
29. Patil, M.; Pabla, N.; Dong, Z. Checkpoint kinase 1 in DNA damage response and cell cycle regulation. *Cell. Mol. Life Sci.* **2013**, *70*, 4009–4021. [CrossRef]
30. Siu, K.T.; Rosner, M.R.; Minella, A.C. An integrated view of cyclin E function and regulation. *Cell Cycle* **2012**, *11*, 57–64. [CrossRef]
31. Wang, Z.; Sun, B.; Zhu, F. Molecular characterization of glutaminyl-peptide cyclotransferase(QPCT)in *Scylla paramamosain* and its role in *Vibrio alginolyticus* and white spot syndrome virus (WSSV) infection. *Fish Shellfish. Immunol.* **2018**, *78*, 299–309. [CrossRef]
32. Murray, T.J.; Yang, X.; Sherr, D.H. Growth of a human mammary tumor cell line is blocked by galangin, a naturally occurring bioflavonoid, and is accompanied by down-regulation of cyclins D3, E, and A. *Breast Cancer Res.* **2006**, *8*, R17. [CrossRef] [PubMed]
33. Denisenko, T.V.; Sorokina, I.V.; Gogvadze, V.; Zhivotovsky, B. Mitotic catastrophe and cancer drug resistance: A link that must to be broken. *Drug Resist. Updat.* **2016**, *24*, 1–12. [CrossRef] [PubMed]
34. Mc Gee, M.M. Targeting the Mitotic Catastrophe Signaling Pathway in Cancer. *Mediat. Inflamm.* **2015**, *2015*, 146282. [CrossRef]
35. Vakifahmetoglu-Norberg, H.; Zhivotovsky, B. The unpredictable caspase-2: What can it do? *Trends Cell Biol.* **2010**, *20*, 150–159. [CrossRef] [PubMed]
36. Vitale, I.; Galluzzi, L.; Castedo, M.; Kroemer, G. Mitotic catastrophe: A mechanism for avoiding genomic instability. *Nat. Rev. Mol. Cell Biol.* **2011**, *12*, 385–392. [CrossRef] [PubMed]
37. Masawang, K.; Pedro, M.; Cidade, H.; Reis, R.M.; Neves, M.P.; Corrêa, A.G.; Sudprasert, W.; Bousbaa, H.; Pinto, M.M. Evaluation of 2′,4′-dihydroxy-3,4,5-trimethoxychalcone as antimitotic agent that induces mitotic catastrophe in MCF-7 breast cancer cells. *Toxicol. Lett.* **2014**, *229*, 393–401. [CrossRef]
38. García, I.A.; Garro, C.; Fernandez, E.; Soria, G. Therapeutic opportunities for PLK1 inhibitors: Spotlight on BRCA1-deficiency and triple negative breast cancers. *Mutat. Res. Fundam. Mol. Mech. Mutagen.* **2020**, *821*, 111693. [CrossRef]